European Journal of Agronomy 100 (2018) 87–98

Contents lists available at ScienceDirect

European Journal of Agronomy

journal homepage: www.elsevier.com/locate/eja

Climate change impact on global potato production

Rubí Raymundo[a,*], Senthold Asseng[a], Richard Robertson[c], Athanasios Petsakos[b], Gerrit Hoogenboom[a], Roberto Quiroz[b], Guy Hareau[b], Joost Wolf[d]

[a] Agricultural & Biological Engineering Department, University of Florida, Frazier Rogers Hall, Gainesville, FL 32611, USA
[b] International Potato Center (CIP), Av La Molina 1895, Lima 12, Peru
[c] International Food Policy Research Institute (IFPRI), Washington, DC, USA
[d] Plant Production Systems Group, Wageningen University, The Netherlands

ABSTRACT

Potato is the most important non-grain crop in the world. Therefore, understanding the potential impacts of climate change on potato production is critical for future global food security. The SUBSTOR-Potato model was recently evaluated across a wide range of growing conditions, and improvements were made to better simulate atmospheric CO_2 and high temperature responses. Comparisons of the improved model with field experiments, including elevated atmospheric CO_2 concentrations and high temperature environments, showed a RRMSE of 26% for tuber dry matter. When using the improved model across 0.5 × 0.5° grid cells over all potato-growing regions in the world, the simulated aggregated country tuber dry yields reproduced nationally-reported potato yields with a RRMSE of 56%. Applying future climate change scenarios to current potato cropping systems indicated small global tuber yield reductions by 2055 (−2% to −6%), but larger declines by 2085 (−2% to −26%), depending on the Representative Concentration Pathway (RCP). The largest negative impacts on global tuber yields were projected for RCP 8.5 toward the end of the century. The simulated impacts varied depending on the region, with high tuber reductions in the high latitudes (e.g., Eastern Europe and northern America) and the lowlands of Africa, but less so in the mid-latitudes and tropical highland. Uncertainty due to different climate models was similar to seasonal variability by mid-century, but became larger than year-to-year variability by the end of the century for RCP 8.5.

1. Introduction

Potato is the most important non-grain crop in the world and the third most important food crop after rice and wheat with an annual production of 330 MT (FAO, 2016). Potatoes are often the main source of income and food security in developing countries (Lutaladio and Castaidi, 2009), and population is increasing in these countries more than any other region in the world (Lutz and Samir, 2010). Climate change could exert acute effects in food supply; therefore, one of the main challenges for modern agriculture is to develop strategies to cope with potential negative impacts of future climate change to ensure food security by 2050 and beyond.

Crop models have been used to study the potential impact of climate change on crop production (White et al., 2011). Crop models integrate the nonlinear dynamics of soil, weather, and crop management to estimate crop growth and production under a wide range of conditions (Jones et al., 2003). Crop models provide a platform to create virtual experiments. For instance, crop models can help to analyze the effect of abiotic stresses during the crop growing cycle or to explore management strategies to improve yields under specific environments (Haverkort and Top, 2011). The vast majority of studies on the impacts of climate change using crop models have focused on grain crops (White et al., 2011). Tubers and roots crops have received little attention, particularly in model testing and model improvement for simulating climate change effects.

Despite little model testing, a range of potato simulation models have been used to study the potential impacts of climate change at local, regional, and global scales (Haris et al., 2015; Franke et al., 2013; Sanabria and Lhomme, 2013; Stockle et al., 2003; Davies et al., 1997). Future projections from potato models have shown that the impacts vary spatially. In some cases, current production areas would shift toward cooler regions (Hijmans, 2003; Supit et al., 2012; Tubiello et al., 2002). Overall, yields would decline by the end of the century, although this decline was higher for models without considering atmospheric CO_2 effects compared with models that include a CO_2 response routine (Raymundo et al., 2014). A model that included a CO_2 routine and an

* Corresponding author. Current address: Department of Agronomy and Plant Genetics, University of Minnesota, 1991 Upper Buford Circle, Saint Paul, MN 55108, USA.
E-mail address: raymundo@umn.edu (R. Raymundo).

https://doi.org/10.1016/j.eja.2017.11.008
Received 11 November 2016; Received in revised form 4 October 2017; Accepted 24 November 2017
Available online 01 December 2017
1161-0301/ © 2017 Elsevier B.V. All rights reserved.

adaptation strategy indicated no change in current levels of potato production in Washington state by 2050 (Stockle et al., 2010). Supit et al. (2012) suggested that in Europe by the end of 2055, the increase of atmospheric CO_2 can mitigate the effect of rising temperature. However, by the end of 2100, the impact of rising temperature may overwrite the positive effect of elevated atmospheric CO_2. In another study, global simulations with a modified version of the LINTUL-potato model indicated yield losses between 18% to 32% by the end of 2050 simulating a single cultivar and assuming no water or nitrogen limitation and no atmospheric CO_2 effects (Hijmans, 2003).

Another potato model, SUBSTOR-Potato has been widely used in simulation studies (Daccache et al., 2011; St'astna et al., 2010; Shae et al., 1999; Mahdian and Gallichand, 1997; Travasso et al., 1996; Brassard and Singh, 2007; Tubiello et al., 2002; Snapp and Fortuna, 2003; Holden et al., 2003; Holden and Brereton, 2006; Stoorvogel et al., 2004). This model considers the growth-stimulating effect of elevated atmospheric CO_2 and the impact of temperature on crop growth and development; however, when compared with a wide range of field data, the model underestimated the impact of elevated atmospheric CO_2 concentrations and could not simulate high temperature effects on crop growth (Raymundo et al., 2016). Therefore, the model needed improvements in simulating responses to elevated atmospheric CO_2 and high temperatures before being applied in climate change impact studies. In this study, our goals are: (a) to report on improvements of the SUBSTOR-Potato model with a range of field experiments; (b) to show how we applied the improved model to estimate the impact of future climate change on global potato production; and (c) to discuss the uncertainty of simulated impact estimates.

2. Materials and methods

2.1. SUBSTOR-Potato model

The SUBSTOR-Potato model is a Cropping System Model (CSM) (Jones et al., 2003) of the Decision Support Systems for Agrotechnology Transfer (DSSAT; Hoogenboom et al., 2015). Griffin et al. (1993), and Ritchie et al. (1995) provide a detailed description of the SUBSTOR-Potato model. The model can be requested from the DSSAT portal (www. DSSAT.net), and the source code is available from GitHub (https://github.com).

The SUBSTOR-Potato model is a process-based model that simulates development, growth, and yield at daily time steps. Crop development and growth are controlled by cultivar parameters including potential leaf growth rate (G2, $cm^2\ m^{-2}\ d^{-1}$), potential tuber growth rate (G3, $g\ m^{-2}\ d^{-1}$), determinacy (PD, dimensionless), effect of photoperiod on tuber initiation (P2, dimensionless), and the effect of temperature on tuber initiation (TC, °C).

The effect of temperature on crop development and growth is described through cardinal temperature functions that simulate the effect of soil temperature on root growth and tuber bulking, the effect of mean temperature on leaf growth, the effect of weighted average air temperature ($0.75*T_{min} + 0.25*T_{max}$) on tuber initiation, and the effect of mean air temperature on carbon fixation or photosynthesis (PRTF).

The daily potential carbon fixation (PCARB) is a function of radiation use efficiency (RUE, $g\ MJ^{-1}$), photosynthetically active radiation (PAR, $MJ\ m^{-2}$), plant density (PLANTS, plants m^2), leaf area index (LAI, dimensionless), and the atmospheric concentrations of CO_2. The actual daily carbon fixation (CARB) is affected by mean air temperature. The effects of atmospheric CO_2 and temperature on carbon fixation are represented by a CO_2 response function (PCO_2, dimensionless) and by a photosynthetic response function to mean temperature (PRFT, dimensionless). PCO_2 is 1 at concentrations of 330 ppm and increases at higher concentrations of atmospheric CO_2.

$$PCARB = RUE*PAR/PLANTS*(1- EXP(-0.55*LAI))*PCO_2 \quad (1)$$

$$CARB = PCARB*PRFT \quad (2)$$

LAI is computed from a potential leaf area (PLA, cm^2). PLA is a function of specific leaf area index ($270\ cm^2\ g^{-1}$) and leaf dry weight (g). In the model, senescence reduces LAI due to age-driven senescence (SLAN, cm^2) or stress (PLASs, cm^2).

Senescence due to stress (PLAS, cm^2) takes place only after tuber initiation and by multiplying the plant leaf area (PLA, cm^2) with the minimum reduction factor of water stress (SLWF), light competition (SLFC), and senescence due to temperature (SLFT). These relative factors range from zero to one.

$$PLAS = PLA*(1.0 - min(SLFW, SLFC, SLFT)) \quad (3)$$

On Eq. (3), the most constraining factor is applied to limit PLAS, ignoring possible interactions of constraining factors. SLFW is a function of water stress. SLFC takes place only when LAI is equal or higher than four. SLFT accounted for the effect of low mean temperature on leaf senescence ($SLFT_{min}$).

The senesced leaf area (DDEADLF, gr) is the maximum factor of SLAN and PLAS divided by the specific leaf area index (LALWR, $270\ cm^2\ g^{-1}$).

$$DDEADLF = max(SLAN, P\ LAS)/LALWR \quad (4)$$

2.2. Model improvement

2.2.1. Experimental dataset

We used free air CO_2 enrichment (FACE) and open top chambers (OTC) experiments conducted by the Changing Climate and Potential Impacts on Potato Yield and Quality (CHIP) project across Europe during 1998 and 1999 to improve the model response to elevated CO_2 concentrations (De Temmerman et al., 2002). We used experiments under contrasting conditions from Peru and the United States to improve the model response to high temperature impacts. In Peru, we used an experiment under high temperature conditions conducted in San Ramon in 2013 in contrast to an experiment under optimum temperature carried out in La Molina during the same year. The same crop management and cultivars were applied in both experiments. In the United States, we used experiments with high temperatures from Washington (1998 and 2003) and Oregon (1988). In San Ramon, Peru, heat stress occurred from emergence to harvest, whereas in Washington and Oregon heat stress occurred after tuber initiation and toward the end of the growing season. Table S1 provides details of the experiments.

Cultivar parameters for these new experiments were based on previous studies with similar cultivars (Raymundo et al., 2016) with some modifications for parameter TC and P2 for cultivars Achirana, Atlantic, Sarnav, and Russet Burbank to better simulate the observed tuber initiation dates. Table 1 shows the cultivar parameters.

Table 1
Crop cultivars coefficients for field experiments.

Country	Representative Sites	G2[a]	G3[b]	PD[c]	P2[d]	TC[e]	Source
Peru	Achirana	2000	21	0.8	0.5	21	(Raymundo et al., 2016)
Peru	Atlantic	1000	25	0.9	0.6	21	(Raymundo et al., 2016)
Peru	Sarnav	1000	30	0.2	0.6	21	(Raymundo et al., 2016)
United States	Russet Burbank	1100	26	0.9	0.2	17	(Hoogenboom et al., 2015)

[a] Leaf expansion rate ($cm^2\ m^{-2}\ d^{-1}$).
[b] Tuber growth rate ($g\ m^{-2}\ d^{-1}$).
[c] Index that suppress tuber growth after tuber induction.
[d] Sensitivity to photoperiod.
[e] Upper critical temperature for tuber initiation (°C).

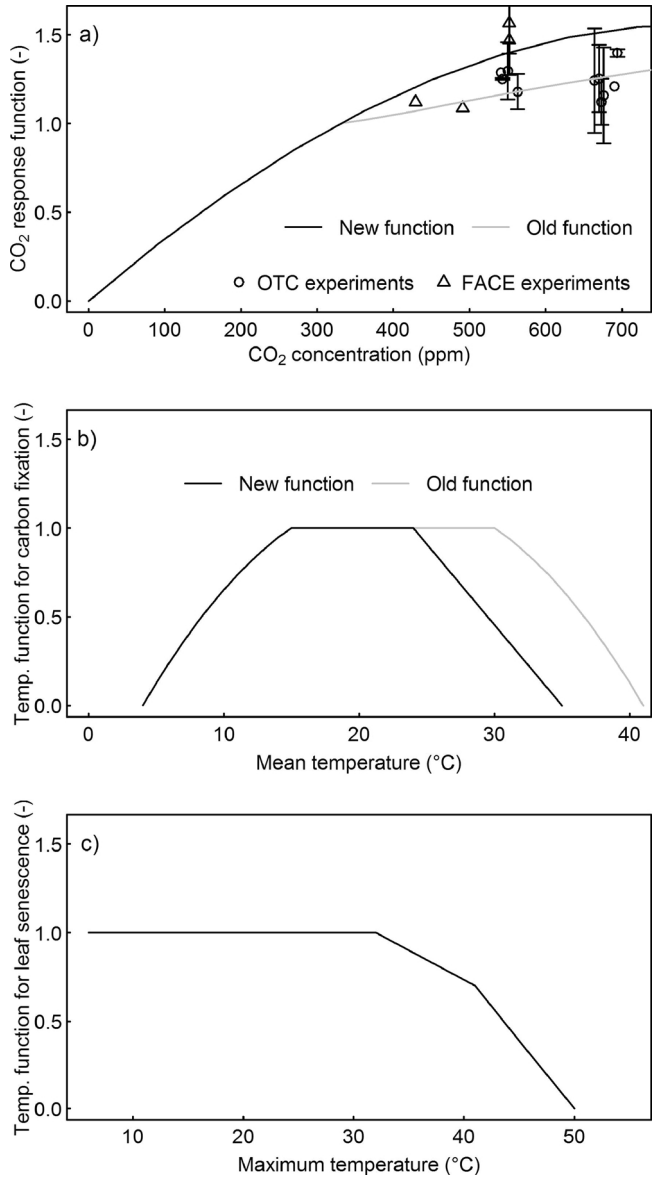

Fig. 1. (a) Modified relative CO_2 response function (PCO_2, −) for carbon fixation in the SUBSTOR-Potato model. Observed relative change of total potato crop biomass due to elevated CO_2 from OTC (○) and FACE (△) experiments (De Temmerman et al., 2002). The relative CO_2 response function (PCO_2) modifies photosynthesis under different atmospheric CO_2 concentrations as a simple multiplier. (b) Modified temperature response functions for carbon fixation (PRFT, −). (c) New response function for accelerating senescence with increasing maximum temperature ($SLFT_{max}$, −).

2.2.2. PCO_2: increase of relative CO_2 response function based on experiments

Based on experimental data (De Temmerman et al., 2002), the original PCO_2 function was increased to reflect the reported potential response of total biomass growth to elevated atmospheric CO_2 (Fig. 1a). To account for the observed stimulated biomass growth at 550 ppm in the FACE experiments at Rapolano Italy, the original CO_2 response function based on previous less responsive experiments (De Temmerman et al., 2002) was modified by increasing the PCO_2 function response parameter from 1.17 to 1.40 at 550 ppm (Fig. 1a). The new parameter in this function has been applied to the simulations of all experiments.

When comparing the SUBSTOR-Potato simulations with observed data of tuber yield, the model showed an increased response to elevated CO_2. In several situations, the response was still less than the observed, especially for the FACE experiments (Fig. 2). A sensitivity analysis (not shown) indicated that for the poorly simulated treatments, N stress occurred earlier during the growing season and consequently simulated N stress restricted the simulated CO_2 response. However, based on the information from these experiments, non-limiting nitrogen were applied in the simulations. While elevated CO_2 stimulates growth, limited N can restrict this effect in reality and in the model. The increased potential CO_2 response function is a general improvement, although N limitations in the model, but not in some of the experiments, are masking the improvements in some cases (Fig. 2). The improved version of the model showed a relative RMSE (RRMSE) for tuber dry weight of 24.3% for FACE and OTC experiments.

2.2.3. PRFT: modification of the photosynthetic response function to temperature

The original temperature function on photosynthesis in the SUBSTOR-Potato model was altered so that PRFT affects the potential carbon fixation (PCARB), instead of the actual carbon fixation (CARB). The old temperature function for photosynthesis (PRFT) was optimal between 15 °C and 30 °C and declined, using a quadratic function, when temperatures were < 15 °C and > 30 °C (Fig. 1b). However, the optimum temperature range was adjusted to be consistent with the approach by Haverkort et al. (2004), with PRFT being optimal between 15 °C and 25 °C (Fig. 1b).

$$PCARB = RUE*PAR/PLANTS*(1- EXP(-0.55*LAI))*PCO_2*PRFT \quad (5)$$

2.2.4. $SLFT_{max}$: heat stress effect on leaf senescence

Another improvement to the SUBSTOR-Potato model included a new relative response function to maximum temperature effects on leaf senescence, based on an approach used for cereals (Asseng et al., 2011) (Fig. 1c), and was added as another factor into equation 6.

$$SLFT = \min(SLFT_{min}, SLFT_{max}) \quad (6)$$

The modified SUBSTOR-Potato model was evaluated with experiments conducted under non-heat stress in la Molina, Peru in 2013 (Fig. 3a) in comparison with heat stress conditions in San Ramon, Peru in 2013 (Fig. 3b) for several cultivars. In San Ramon, the maximum and minimum temperatures were frequently above 30 °C and 20 °C, respectively. Under non-heat stress conditions, the model improvements did not affect the simulation results for tuber dry weight and aboveground biomass, but reduced growth closer to the observations under high temperatures at San Ramon.

In temperate regions, heat stress can occur after tuber initiation toward the end of the growing season, with maximum temperatures above 30 °C, but minimum temperatures at the same time not exceeding 20 °C. For field experiments in a temperate environment at Washington, USA and Oregon, USA, the model with the modified temperature routines simulated aboveground and tuber dry weight well (Fig. 4d–f), with a RRMSE of 13.4% for aboveground dry weight and 25.4% for tuber dry weight.

2.3. Global simulations

2.3.1. Global crop potato area

Three global geo-referenced datasets of global potato production areas are available (You et al., 2014; Monfreda et al., 2008; Hijmans, 2001). For this study, we used the Spatial Production Allocation Model (SPAM) dataset (You et al., 2014) as this one distinguishes between irrigated and rainfed potato cropping systems. However, when compared with the world potato atlas (https://research.cip.cgiar.org/confluence/display/wpa), the SPAM dataset underestimated total irrigated potato areas for some countries and was therefore corrected for India (from 50% to 80%), South Africa (from 0% to 85%), Canada (from 0% to 18%), Iraq (from 0% to 50%), Nepal (from 0% to 50%), Turkey (from 0% to 50%), Thailand (from 0% to 50%), and Cyprus (from 0% to

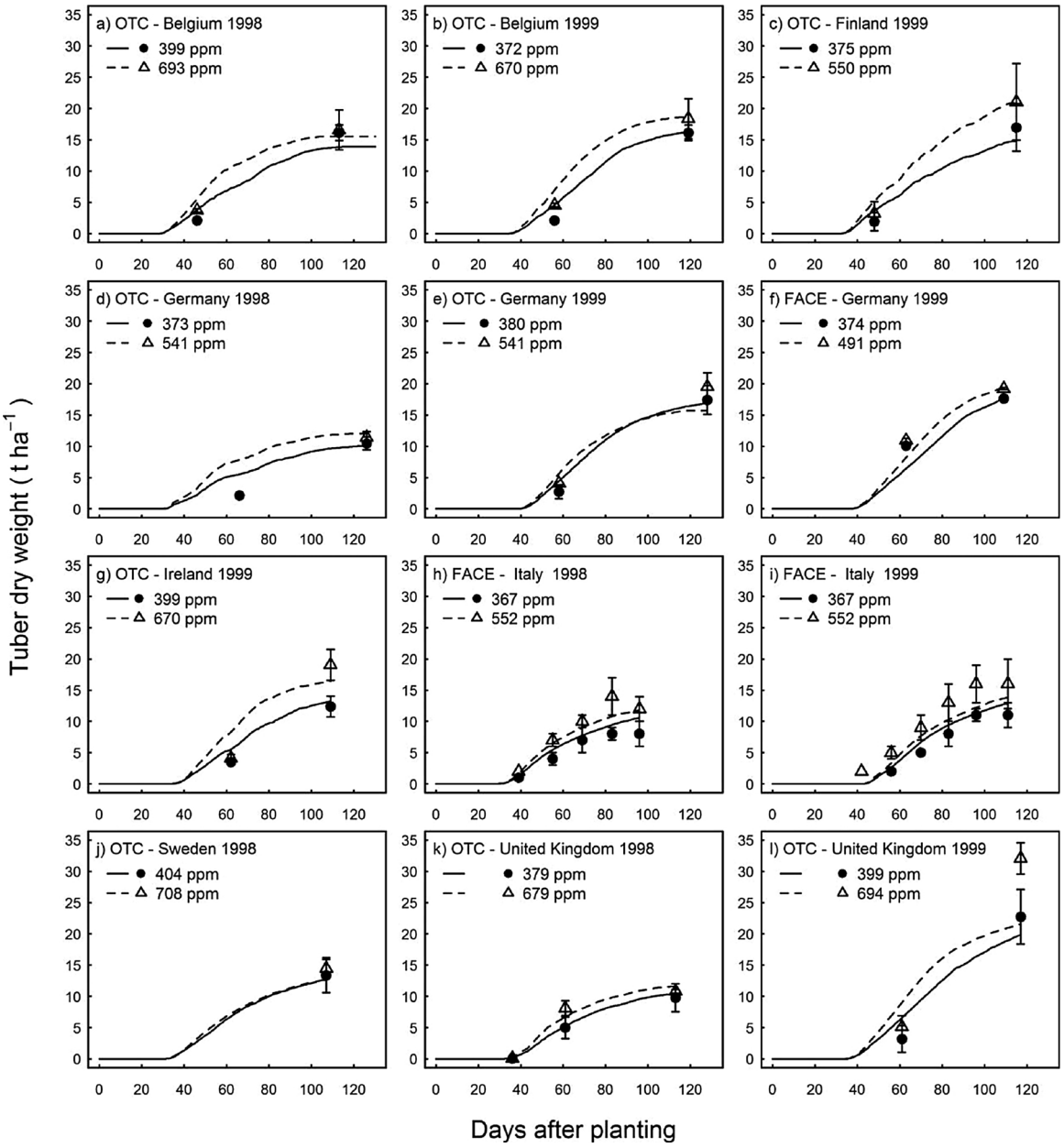

Fig. 2. Observed versus simulated potato tuber dry weight (t ha^{-1}) for ambient (●, –) and elevated atmospheric carbon dioxide (△,—) using a new CO_2 response function from Fig. 1a. Observed data from OTC and FACE experiments (De Temmerman et al., 2002).

100%).

2.3.2. Climate data

For our climate change impact study, we used one recent global historical period (1979–2009) as the baseline and two future periods, 2040–2070 (2055) and 2071–2100 (2085), and two Representative Concentration Pathways (RCPs), 4.5 and 8.5.

Daily temperatures, solar radiation, and precipitation were from the NCEP/NCAR reanalysis database (Kalnay et al., 1996). The original spatial resolution of the NCEP data is about 1.884° N/S and 1.865 E/W. The precipitation values were from the Global Precipitation Climatological Center (GPCC; http://www.esrl.noaa.gov/psd/data/gridded/data.gpcc.html) for the same time periods at a 0.5 × 0.5° resolution. For each location, the daily NCEP-derived data within a particular month were scaled up or down so that the total for the entire month matched the value in the higher-spatial/lower-temporal resolution GPCC dataset. Based on these maps (temperatures and sunshine at coarse spatial resolution and adjusted rainfall at finer resolution), weather files were generated at 0.5° resolution, taking the values for each variable from whichever pixels they fell. This approach provided the 'baseline' or historical weather data.

Five downscaled and bias-corrected Global Circulation Model (GCM) scenarios (HadGEM2-ES, IPSL-CM5A-LR, GFDL-ESM2M, MIROC-ESM-CHEM and NorESM1-M) were obtained from ISI-MIP (the Inter-Sectoral Impact Model Intercomparison Project) database (revised version from November 2015) from the Potsdam Climate Institute (PIK). The data include daily weather values over the period 1960–2099 derived from five climate models, and four representative concentration pathways (RCPs). A more detailed description of these data can be found in Mueller and Robertson (2014). From these daily values, monthly averages for the pertinent variables were extracted for 30-year windows: 1979–2009 representing the recent past, 2041–2070 representing the anticipated mid-century conditions, and 2071–2099 for late century.

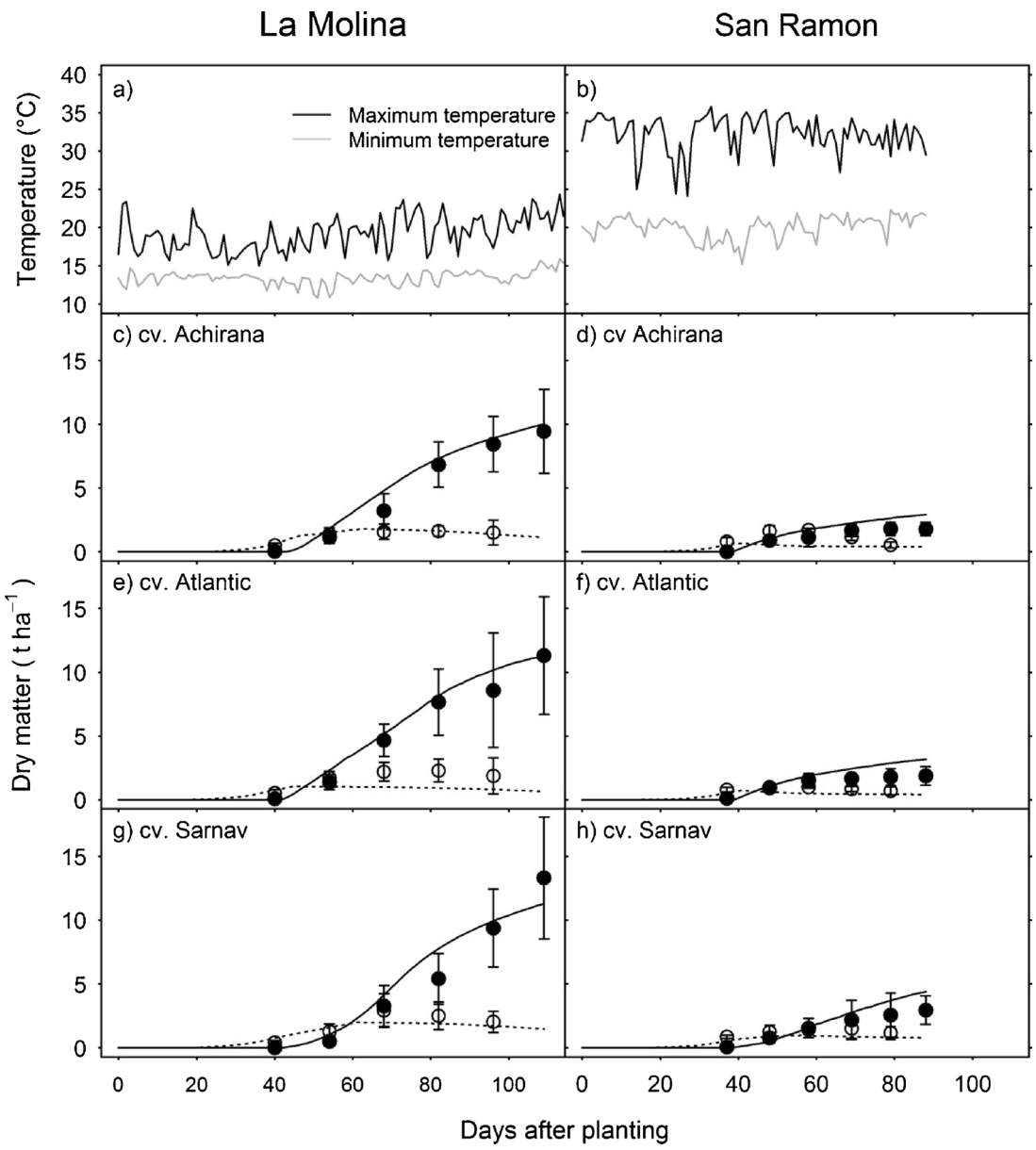

Fig. 3. Minimum (gray lines) and maximum temperature (black lines) for a non-heat stress environment and a heat stress environment: (a) La Molina and (b) San Ramon respectively, Peru, 2013. Observed versus simulated potato tuber dry weight (t ha^{-1}) (●, –) and aboveground dry weight (t ha^{-1}) (○,—) for (c and d) cv. 'Achirana', (e and f) cv. 'Atlantic', and (a and h) cv. 'Sarnav' using new temperature response functions from Fig. 1b and 1c. Error bars indicate standard error of measurements when available.

The changes in the climate embodied in the time-slice averages were applied to the daily climate of the historical weather data (or to the baseline) to create future weather data for the simulations. The new daily value of temperature is the old daily value plus the difference between the future monthly value and the historical monthly value from the GCMs. Solar radiation was bounded by zero, so the values are scaled; the new daily value is the old daily value multiplied by the ratio of the future and historical monthly values. Rainfall is handled similarly per day.

2.3.3. Mega-environments

To cover all potato growing regions of the world, the climate classification (e.g., temperate, subtropics, and tropic) was used from the FAO Global Agro-Ecological zones (Fischer et al., 2002). In the tropical and subtropical regions, a digital elevation model (http://www2.jpl.nasa.gov/srtm/) assisted in discriminating between the lowlands and highlands. Photoperiod has a direct effect on tuber initiation, and this response can vary across cultivar and species. Cultivars adapted to long photoperiod (> 12 h) with neutral response to photoperiod are planted across the temperate region. Cultivars adapted to short photoperiod are restricted to the subtropics and tropic (< 12 h) (Mendoza and Haynes, 1976). In the temperate region, cultivars were grouped in temperate neutral photoperiod (12 to < 15 h) and temperate long photoperiod (> 15 h) requirements. The corresponding photoperiod for the temperate region was calculated starting at one month after the planting when tuber initiation usually occurs (Streck et al., 2007; Singh et al., 2005).

The classification described above resulted in six mega-environments (Fig. 5). Each region was assigned a cultivar with a parameter set for the SUBSTOR-Potato model and a specific length of growing season (Hoogenboom et al., 2015; Kleinwechter et al., 2016) (Table 2).

2.3.4. Soil data and initial conditions

Global soils and initial soil conditions were obtained from Gbegbelegbe et al. (2016). The soils were from the geo-referenced HC27 generic soil profile database created by Koo and Dimes (2015).

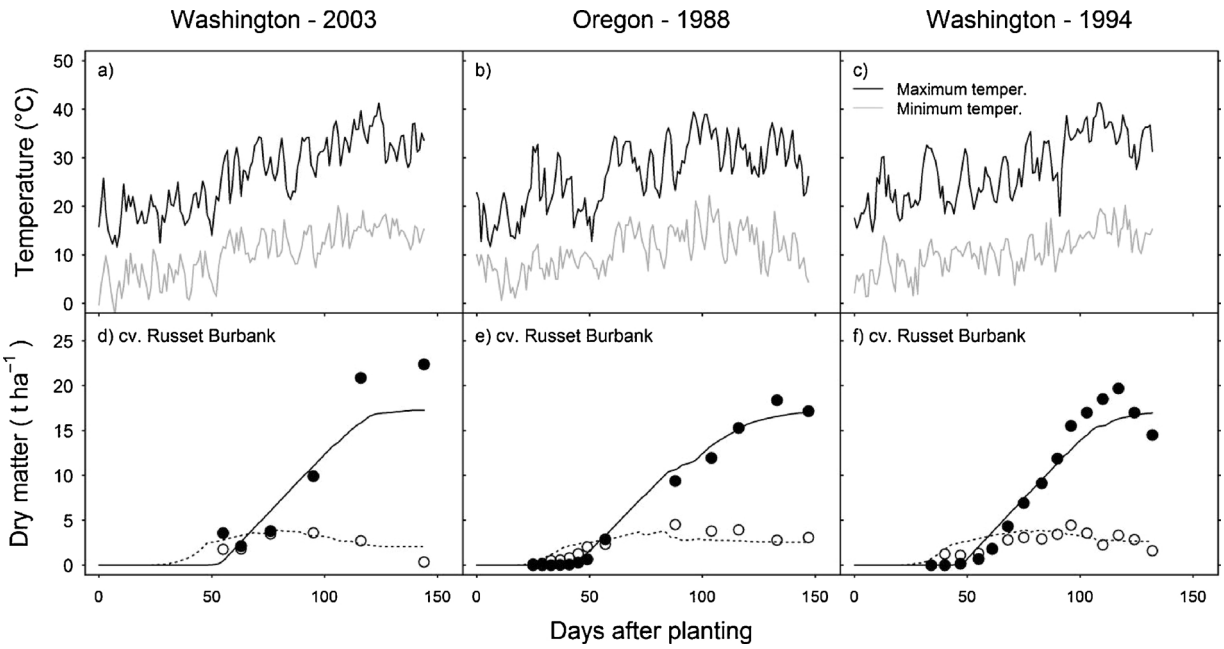

Fig. 4. Minimum (gray lines) and maximum temperature (black lines) for location in (a, c) Washington and (b) Oregon, USA. Observed versus simulated potato tuber dry weight (t ha^{-1}) (●, −) and aboveground dry weight (t ha^{-1}) (○,—) for (d, e and f) cv. 'Russet Burbank' using new temperature response functions from Fig. 1b and 1c.

This database has 27 generic soil profiles based on all combinations of three organic carbon levels (high, medium, low), depths (shallow, medium, deep), and major texture types (clay, loam, sand). The map of locations was built based on the Harmonized World Soil Database by applying thresholds to the appropriate soil characteristics to classify them into the 27 generic types. The initial soil conditions include initial surface residue, initial soil organic carbon, initial water content (mm), and initial mineral soil nitrogen (kg ha^{-1}). The initial soil water content was defined at 25% between the lower limit of plant extractable soil water and the drained upper limit.

2.3.5. Planting dates

Planting dates were defined using threshold temperatures and geo-referenced monthly temperature data (Hijmans et al., 2005). Minimum temperature thresholds for tuber initiation and tuber bulking range from 4 °C to 18 °C (Griffin et al., 1993), and the maximum temperature threshold for optimum crop development is < 30 °C (Hammes and Dejager, 1990). A planting month was selected when the threshold temperatures were met for three consecutive months. In locations where temperatures were suitable for growing potato year-round (e.g., highlands of South America and Africa), monthly precipitation was used in addition to determine a planting month. If > 300 mm and < 800 mm of rainfall occurs in average in three consecutive months, the first of these three months was used as a planting month. As there is little irrigation in the tropics, the same planting date was applied even when irrigation occurred (Fig. S1e).

2.3.6. Fertilizer application

Geo-referenced nitrogen application rates (kg ha^{-1}) for potato (Mueller et al., 2012) were disaggregated for rainfed and irrigated systems by assigning the reported maximum value to irrigated systems and the reported minimum value to rainfed systems. In cases where the maximum and minimum values were similar and the nitrogen was higher than 150 kg ha^{-1}, two-thirds of the nitrogen application was assigned for rainfed systems. When the nitrogen application was less than 150 kg ha^{-1}, a third of this amount was added and used as the nitrogen fertilizer amount for irrigated systems. For locations with no data, we assigned default values of 60 kg ha^{-1} for rainfed and

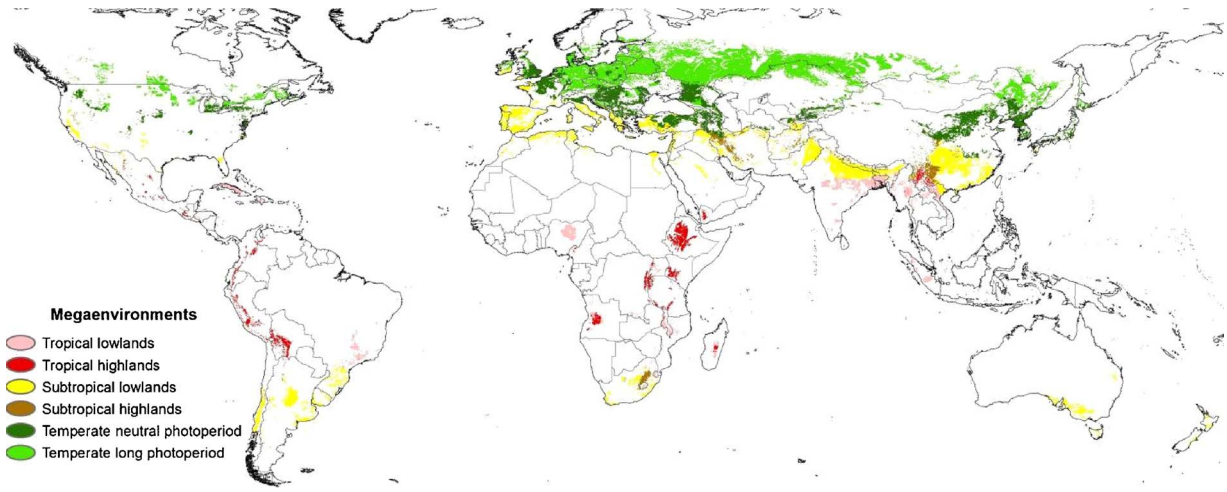

Fig. 5. Potato mega-environments for global SPAM (You et al., 2014) potato production.

Table 2
Coefficients for each potato cultivar representing apotato Mega-Environment (ME).

Mega-Environment	Representative Sites	Benchmark Cultivar	G2[a]	G3[b]	PD[c]	P2[d]	TC[e]	Source
Temperate long photoperiod	Oregon, USA	Russet Burbank	1100	26	0.9	0.2	17	(Hoogenboom et al., 2015)
Temperate neutral photoperiod	Rapolano, Italy	Bintje	1000	30	0.8	0.1	19	(Raymundo et al., 2016)
Subtropical highland		LT1	2000	25	0.9	0.8	17	(Hoogenboom et al., 2015)
Subtropical lowland	Modipuram, India	KufriBahar	2000	22	0.9	0.8	23	(Kleinwechter et al., 2016)
Tropical highlands	Huancayo, Peru	Amarilis	2000	30	0.9	0.9	20	(Kleinwechter et al., 2016)
Tropical lowlands	Lima, Peru	Achirana	2000	21	0.8	0.5	21	(Raymundo et al., 2016)

[a] Leaf expansion rate ($cm^2\ m^{-2}\ d^{-1}$).
[b] Tuber growth rate ($g\ m^{-2}\ d^{-1}$).
[c] Index that suppress tuber growth after tuber induction.
[d] Sensitivity to photoperiod.
[e] Upper critical temperature for tuber initiation (°C).

120 kg ha^{-1} for irrigated systems. An optimum level of nitrogen rate application (~200 kg ha^{-1}) was defined for countries where potato production relies exclusively on irrigation.

2.3.7. Global simulations

The DSSAT software was linked to the Geographic Resources Analysis Support System (GRASS) Software v. 6.4 (GRASS, 2012) for global gridded simulations. Geo-referenced layers of initial conditions, crop management, soil profiles, planting dates, and mega-environments were the same for baseline and future simulations. Simulations for the irrigated regions used automatic irrigation. Evapotranspiration was calculated with the Priestley-Taylor equation (Priestley and Taylor, 1972). Soil water infiltration was computed with the capacity approach method. Soil evaporation was estimated with the Suleiman-Ritchie method (Suleiman and Ritchie, 2003), and the dynamics of carbon and nitrogen were simulated with the CENTURY model (Hoogenboom et al., 2015). For baseline simulations (1979–2009), atmospheric CO_2 levels were 379 ppm. For future conditions, atmospheric CO_2 levels based on RCP 4.5 for 2041–2070, RCP 8.5 for 2041–2070, RCP 4.5 for 2071–2100 and RCP 8.5 for 2071–2100 were 498 ppm, 572 ppm, 532 ppm and 802 ppm, respectively (IPCC, 2013).

All simulations started 90 days before planting to consider rainfall effects on soil water conditions. Simulations were carried out for each grid cell from 1979 to 2009 for rainfed and irrigated conditions. The simulated yields were multiplied by rainfed and irrigated area per grid cell. Potato yields were reported as the mean of 30 years comprising area-weighted averages for rainfed and irrigated yield for each grid cell. Cultivars were assigned to each grid cell based on mega-environments. To evaluate the performance of the crop model at a global scale, the simulated and reported tuber dry weights were compared for ten years (2000–2009), assuming little technology trend in the observed data during this period. Baseline simulations under irrigated and rainfed conditions were aggregated at the country level to determine the area-weighted average tuber yield per country. Reported yields of tuber fresh weight (t ha^{-1}) were obtained from FAOSTAT website (FAO, 2016). To compare simulated with FAO reported yields at the same tuber moisture content, the FAO reported tuber fresh weights were converted to dry weight by multiplying reported fresh weights with a factor of 0.2 (i.e. assuming a dry weight of 20%). Comparisons of simulated and FAO yields were then made for all countries (104) that had reported potato acreage greater than 5000 ha and SPAM pixels with more than five ha.

Simulated tuber yields were averaged for each RCP and future time slice. To determine the expected change in yield, we calculated the relative difference of simulated yields between 2041 and 2070 and 1979–2009 (baseline) and between 2071 and 2100 and 1979–2009 (baseline) for each RCP (4.5 and 8.5). We calculated uncertainty for GCM scenarios (spread of simulated yields due to differences in GCMs) and quantified simulated variability between years (30 years). The uncertainty and the year-to-year variability of future yield projections were quantified by standard deviations. Groups of uncertainty and variability were defined as low, medium, and high. The combination of uncertainty and variability produced nine groups to categorize results as low-low, low-medium, low-high, medium-low, medium-medium, medium-high, high-low, high-medium, and high-high.

3. Results

3.1. Global baseline simulations

Global simulations with the improved SUBSTOR-Potato model were averaged over 30 years (1979–2009) and weighted for irrigated and rainfed contributions for each pixel across the world (Fig. 6). The simulated potato tuber dry yields ranged from 1 to 18.5 t ha^{-1}. The highest simulated yields occurred in the temperate regions of North America and Europe, whereas yields were low in most tropical and subtropical regions. The annual variability (data not shown) ranged from 0.1 to 6.5 t ha^{-1}. This variability was higher than 1.0 t ha^{-1} for North America, Europe, North Asia, and the highlands of South America, and less than 1.0 t ha^{-1} for central Asia and Africa. Regions with low simulated yields (< 3 t ha^{-1}) often had higher relative variability (data not shown).

Fig. 7 shows the simulated mean of 10 years potato country yields and production compared with the mean of 10 years reported country data. The error bars of the mean indicate the annual simulated (vertical) and observed (horizontal) variability. The annual variability of individual country tuber yields was higher for simulated yields than for reported yields. The spread of data around the 1:1 line for yields was large, but less for country production, except for the two largest potato producers, China and Russia. For Russia, the simulated yield was almost twice as high as the reported yield. Yields were underestimated for Cuba, Philippines, Indonesia, and Guatemala. On average, the comparison of simulated and reported country tuber dry yield resulted in RRMSE of 56%.

3.2. Impact of climate change

Fig. 8a shows the relative impact of climate change on potato production by 2055 for RCP8.5. For this emission scenario, the model projection indicated yield reductions for the temperate regions of North America, Eastern Europe, and Asia, and a yield increase for Western Europe. For the subtropical and tropical regions, the model projected an increase in tuber yield in the Indo-Gangetic Plain, and the highlands of South America, Africa, and Asia. Across the five GCMs, the most pessimistic projection was with HadGEM2-ES, while GFDL-ESM2M had the most optimistic (Fig. S2). Geographic patterns for GFDL-ESM2M were opposite in many regions to other GCMs for both RCPs and time periods (Figs. S5–S8).

For the RCP 8.5 projection for 2055, the uncertainty of tuber dry yield based on the five GCMs, ranged between 0.1–5.5 t ha^{-1}, and the

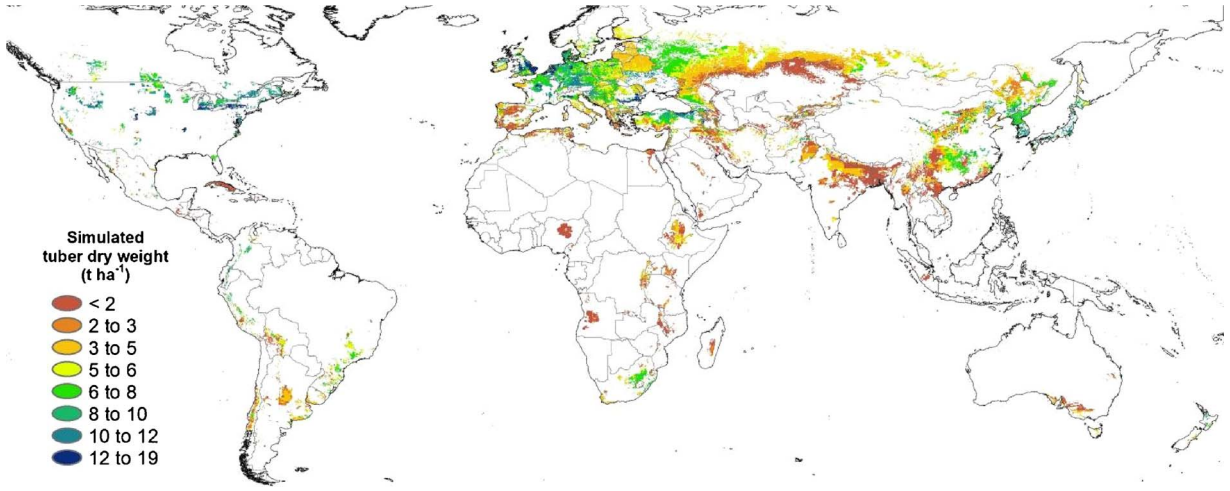

Fig. 6. Simulated average (1979–2009) global potato dry tuber yields for 0.5 × 0.5° grid cells. Potato tuber yields in each pixel are simulated weighted averages for rainfed and irrigated production.

inter-annual variability of tuber dry yield based on 30 years of simulations ranged from 0.1 to 6.2 t ha^{-1}. The uncertainty and the annual variability were classified into three groups: low (0.1–1.0 t ha^{-1}), medium (1.0–2.0 t ha^{-1}) and high (2.0–6.2 t ha^{-1}). In most regions of the world, the inter-annual variability was larger than the uncertainty from the GCMs (Fig. 8b). In the temperate region, uncertainty and variability were high (North America), medium-high (Central Europe), and medium-medium (Eastern Europe). In the subtropical and tropical regions, uncertainty and variability were low-medium and low-high. Regions with large yield reductions due to climate change in the temperate region coincided with large GCM uncertainty and large annual variability (Fig. 8b). Large annual variability is often driven by climate extremes which are also more difficult to project with GCMs.

The geospatial pattern of yield change due to climate change based on RCP 4.5 for 2055, RCP 8.5 for 2055, and RCP 4.5 for 2085 were similar (Fig. S2). However, yield losses were lower for RCP 4.5 (Fig. S2). Yields declined for most of the world by 2085 for RCP 8.5, except for some regions in the central highlands of South America, the subtropical highlands, the Indo-Gangetic Plain, and Central China (Fig. S2). By the end of the century (2085, RCP 8.5), the uncertainty due to GCM was greater than the inter-annual variability for the temperate regions, the Northern Andes of South America, and some regions of Africa and China (Fig. S3). Globally, projections with RCP 4.5 indicated that global tuber yields will decline by 2.1% and 1.8% by 2055 and 2085, respectively. For RCP 8.5, the projections indicated a global tuber yield decline of 5.6% and 25.8% by 2055 and 2085, respectively (Fig. 9). To judge the relative magnitude of GCM, we compared this with annual variability. The GCM uncertainty in this study was relatively large. It was as large as annual variability for both RCPs for 2055, but uncertainty from GCMs became even larger than the year-to-year variability for RCP 8.5 by 2085, hence the late century results should be used with caution.

4. Discussion

The SUBSTOR-Potato model is one of the most widely used potato models. However, a comprehensive recent model testing with detailed field experimental data revealed shortcomings in simulating the impact of elevated atmospheric CO_2 and high temperatures, but performed well in simulating the effects of irrigation, N-fertilizer, and cultivar

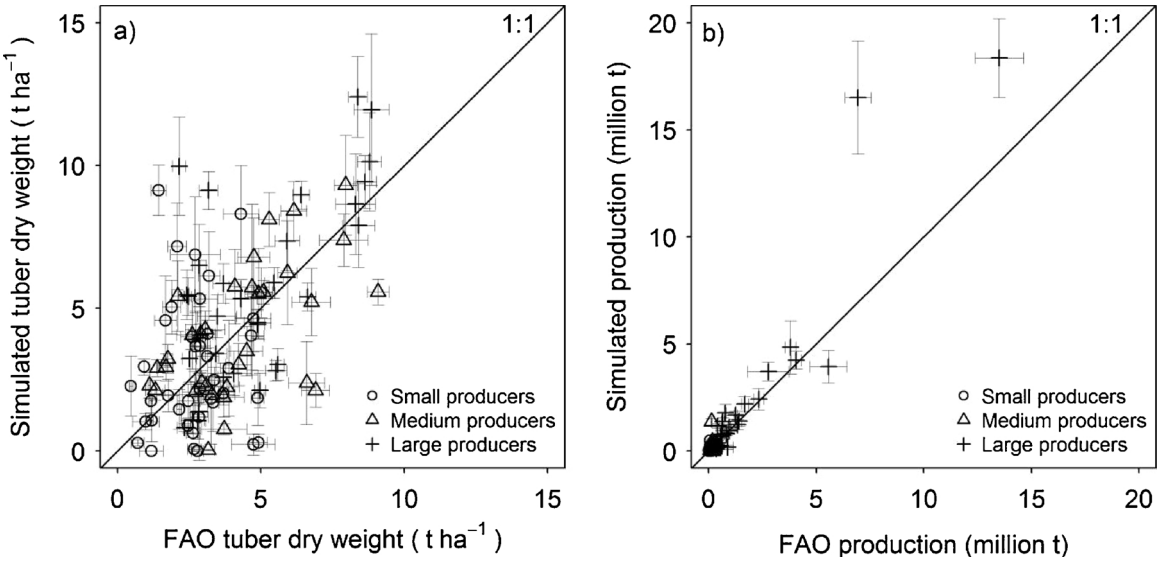

Fig. 7. Simulated versus observed (a) country potato dry tuber yields (t ha^{-1}) and (b) country potato dry tuber production (million t) for 104 countries for the period 2000–2009. Observed country yields are from the Food and Agriculture Organization (FAO, 2016). Potato-producing countries were grouped into small (< 0.5 million t), medium (> 0.5 to < 1.7 million t) and large (> 1.7 million t) potato-producing countries (annual dry tuber production). Error bars indicate standard deviations for ten years of simulated and reported yields.

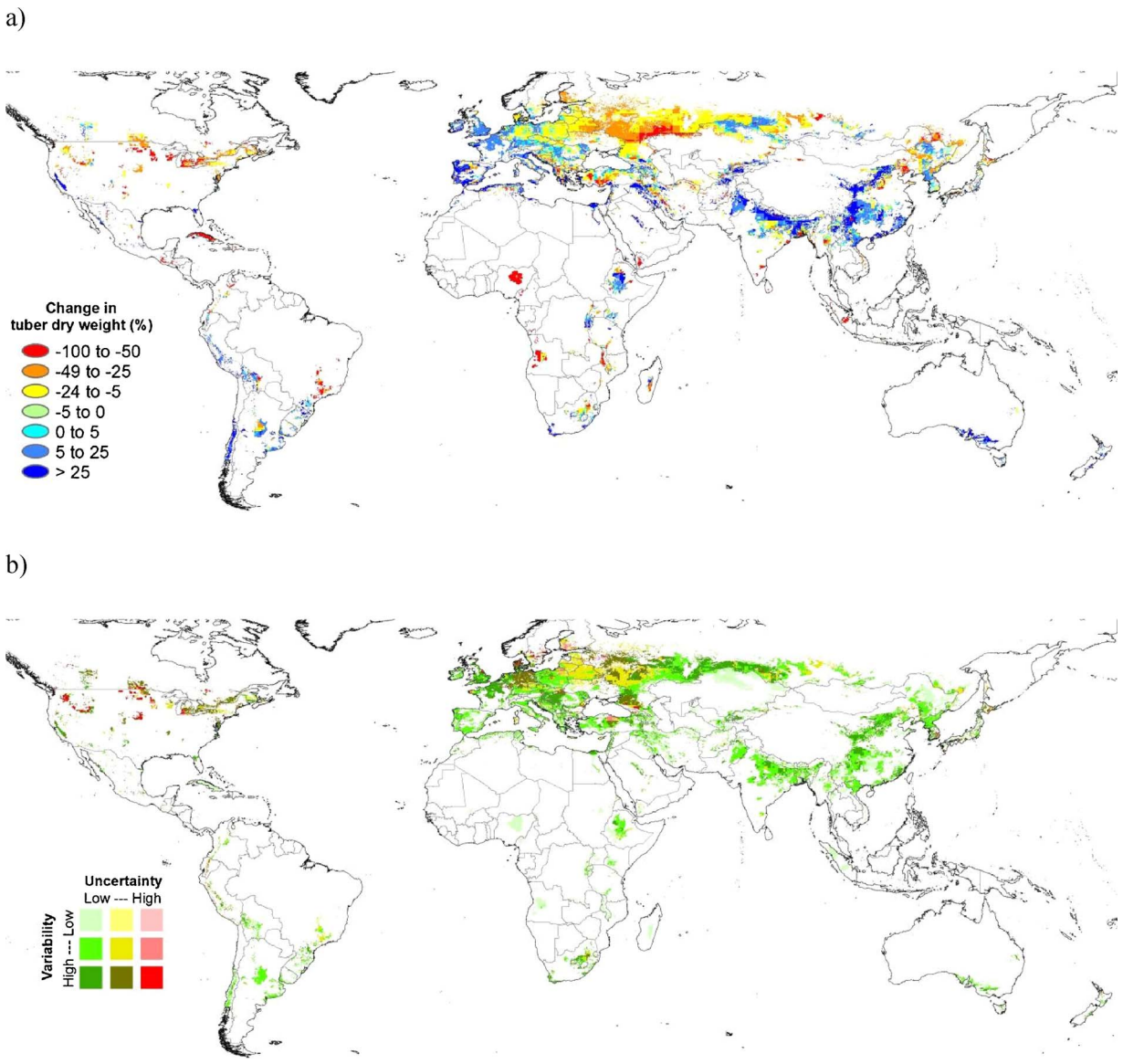

Fig. 8. (a) Simulated average relative change in potato dry tuber yields (%) for RCP 8.5. and 2040–2070, compared to 1979–2009. The simulated relative change in yields is the mean of five GCMs and 30 years. (b) Uncertainty, calculated from five GCMs vs. inter-annual variability across 30 years (both calculated as standard deviation) of simulated yields (for ranges of 0.1–1.0 t ha^{-1}, 1.0–2.0 t ha^{-1} and > 2 t ha^{-1} yield changes).

differences in many different environments (Raymundo et al., 2016). Raymundo et al. (2016) identified shortcomings in simulating the response to elevated CO_2 and high temperatures. An improved physiological understanding of crop responses to elevated CO_2 and high temperatures was included into the model. These improvements allowed the model to simulate tuber yield in a range of field experiments with elevated CO_2 and high temperatures. The model was later applied to assess the impact of climate change at a global scale. However, more model improvements could be possible regarding elevated CO_2, but field data for this is often limiting. For example, stomatal resistance increases with elevated atmospheric CO_2 concentrations, which in turn increases canopy temperature, causing an amplification of leaf senescence and possibly reducing the length of the growing period (Magliulo et al., 2003). Such a process is currently not considered in the SUBSTOR-Potato model. Improving high temperature effects on crop growth and in particularly on senescence, has been shown to be critical for simulating heat stress in other crops (Liu et al., 2016). The inclusion of a modified heat stress function from wheat, accelerating senescence under high maximum temperatures (Asseng et al., 2011) into the SUBSTOR-Potato model, has improved the simulation of potato growth, LAI and tuber yield in environments where high temperatures are frequent.

The improved SUBSTOR-Potato model was then used to simulate potato production across the globe. Simulated, aggregated yields and production were compared with country records for 104 countries. This comparison showed a RRMSE for tuber yields of 56%, which is higher than when the same model was tested with individual field data from many environments across the world with a RRMSE of 37% (Raymundo et al., 2016). There could be several reasons for the larger RRMSE at the country level. Input information is usually of much poorer quality for 0.5 × 0.5° grid cells compared to well-documented field experiments. For example, the frequent SPAM irrigated-to-rainfed area ratio differed for some regions in comparsion with other references, suggesting some uncertainty with this specific database (Siebert et al., 2015). Another source of error is the resolution of weather data, which could be too broad in terrain with changes in elevation or close to coastlines. The used reanalysis data had been shown to adequately represent local conditions (Kalnay et al., 1996); however, the resolution was clearly inadequate in coastlines and mountain ranges. For example, potato yields were underestimated in coastal regions of Cuba, Philippines, and

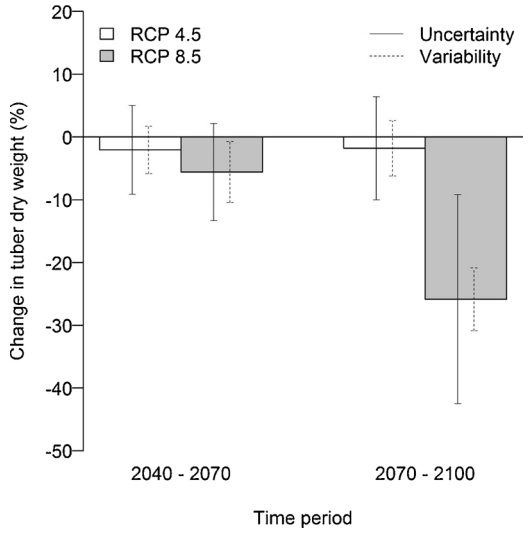

Fig. 9. Simulated global mean relative change in potato tuber dry yields for 2041–2070 and 2071–2100 for RCP 4.5 and 8.5. Error bars represent standard deviation of five GCMs (solid line error bars, GCM uncertainty), and 30 years (dotted line error bars, natural or year-to-year variability).

Indonesia, where the grid cell often represented a part of an ocean. This was indicated by a narrow diurnal temperature range and too high minimum temperatures. In these cases, the model could not simulate tuber initiation and tuber bulking correctly. The model also underestimated tuber yields for Guatemala, where excessive rainfall triggered nitrogen leaching resulting in N shortage and low tuber yields. An overestimation of yield occurred in some regions where pest and diseases were often not controlled adequately. For example, in Russia, there are reports of poor seed potato quality and less control of diseases, often resulting in low potato yields (Haase and Haverkort, 2006; Islamov, 2005). In addition, the choice of the grid cell size also contributes to the simulated impact uncertainty (Zhao et al., 2016). And, the quality of FAOSTAT reported yields, often varying among countries, could be another source of error in such a model-observation comparison. In fact, part of the FAO data are estimates, rather than farmers' reports (FAO, 2016). However, the country yield testing with the SUBSTOR-Potato model was similar to another study in Europe with LINTUL-FAST with a RRMSE of 52% (Angulo et al., 2013), while other global or regional studies did not attempt to evaluate large-scale simulations with any regional observations (Supit et al., 2012; Hijmans, 2003).

The global climate change impact simulations suggested small reductions of potato yields by 2055, but up to a 26% potato yield decline towards the end of the century for a RCP 8.5 scenario. A critical aspect of our global impact estimates is considering the complexity of water and N limitations in different potato cropping systems and their interactions with regional specific cultivars, climate variability and climate change. For example, the elevated atmospheric CO_2 growth stimulus was shown to be larger under non-water limiting growing conditions (e.g. in high rainfall regions or under irrigation), but was negligible if N was limiting growth (e.g. in low input, rainfed cropping systems). Considering such interactions in the global study with the SUBSTOR-Potato model explains some of the differences in results of climate change impacts when compared to other global estimates where water and N were wrongly assumed to be global/regional not limiting (Hijmans, 2003; Supit et al., 2012; Angulo et al., 2013). Considering water and N limitations in models results in more realistic climate impact estimates (Webber et al., 2015), suggesting that potato tuber yields will increase by midcentury only for western Europe and yield will decline for most of eastern Europe. In contrast, Angulo et al. (2013) used a non-water and non-N limited crop model and showed that potato yields increased for most of Europe. Another study by Hijmans (2003) using the LINTUL-potato model suggested a decline in global potato yields between 18% and 32% by 2050. However, in their study, potato simulations were conducted outside the main areas currently identified by the SPAM database for potatoes. The additional areas in the simulations might have contributed to the larger suggested yield decline in the Hijmans (2003) study. Some of the differences in impact simulations are due to considering different growth factors, including water and N (Webber et al., 2015), and elevated atmospheric CO_2, but simulated differences can also be due to general differences in potato crop models (Fleisher et al., 2016). Fleisher et al. (2016) showed with a multi-model ensemble of potato crop models that impact model uncertainty increased to 41% with increasing temperatures alone. A similar increase in impact model uncertainty with rising temperatures has been reported for other crops (Asseng et al., 2015; Bassu et al., 2014; Li et al., 2015). However, crop model uncertainty is likely to be larger than climate projection uncertainty from GCMs as shown for wheat by Asseng et al. (2013).

Since 2005, potato-producing areas have declined in temperate regions due to changing nutritional demands. However, potato-producing areas have increased in most developing countries (Lutaladio and Castaidi, 2009), in areas with high poverty rates, and in regions with agriculture as a main economic activity. Hotspots of high poverty rates and production systems based on potato crops are located in the Andes of South America, Sub-Saharan Africa and the Asian Pacific (Theisen and Thiele, 2008). However, by 2050, climate change impact projections indicated more optimistic results for these regions. For example, impact projections for India suggested little yield changes or even an increase in some areas, if water remains available for irrigation. A slight yield increase occurred as temperature conditions became more suitable for potatoes. In the highlands of South America and the tropics and subtropics of Asian Pacific, simulated impacts suggested a yield increase also under rainfed production systems. This yield increase occurred due to sub-optimal temperatures becoming more optimal with warming at higher elevations. Therefore, potato production will continue to be a viable option to maintain food supply in these poverty-affected regions by midcentury. However, the simulation results indicated large negative yield impacts with climate change in the lowlands of Sub-Saharan Africa with yield reductions of up to 50% by midcentury. For example, Nigeria is the top potato-producing country in Sub-Saharan Africa, and has doubled potato production by cropping more land with potatoes since 2000 (Devaux et al., 2014). However, simulated future potato tuber yields in Nigeria are suggested to decline across the country, at the same time, population across Africa is likely to double by midcentury (Cleland, 2013). Despite possible increases in potato-growing areas, regional food demand is likely to grow faster than regional production in Sub-Saharan Africa.

Strategies to mitigate climate change vary across regions because climate change has different regional impacts on agricultural production. Regions with possible yield increases with climate change, mostly in developing countries, are an opportunity to further increase crop production without additional land. Regions with suggested yield declines from climate change, such as the lowlands of Sub-Saharan Africa, will require specific crop adaptations to rising temperatures by switching to more heat-tolerant potato cultivars (Adhikari et al., 2015) or even considering other crops for food supply (Jarvis et al., 2012). Adaptation strategies need to be explored to ensure future food security, particularly in high population growth regions where demand is likely to outpace production.

5. Conclusions

A comprehensive climate change impact simulation for global potato production showed less pessimistic yield changes than previous studies, but still indicate large yield declines for most regions of the world toward the end of the century under high emission scenarios. The

magnitude of uncertainty for RCPs and GCMs increased towards the end of the century, and areas with large simulated yield losses coincided with high natural variability, but also high impact estimate uncertainty. Regions with large year-to-year variability are already exposed to large climate variability causing low yields in some seasons. Climate change increases variability, but uncertainty is also large, partly due to GCM scenario uncertainty for these regions and partly due to crop model uncertainty in simulating large variability in growing conditions. The regions that most depend on potato production for food security are also regions least able to invest themselves in agriculture and are the hardest hit by climate change impacts. These regions will require outside assistance for region-specific adaptations to climate change.

Acknowledgements

Funding support for the global modeling aspects of this research was provided by the Global Futures and Strategic Foresight project of the CGIAR Research Program on Policies, Institutions, and Markets (PIM). We thank the International Research Food Policy Research Institute (IFPRI) and the USAID Linkage Fund project "Collaboration between the International Potato Center (CIP) and the University of Florida (UF) to better understand and prioritize climate change adaptation needs for food security in the Andes". We thank Patrick Ray for assisting with global climate data.

Appendix A. Supplementary data

Supplementary data associated with this article can be found, in the online version, at https://doi.org/10.1016/j.eja.2017.11.008.

References

Adhikari, U., Nejadhashemi, A.P., Woznicki, S.A., 2015. Climate change and eastern Africa: a review of impact on major crops. Food Energy Secur. 4 (2), 110–132.
Angulo, C., Rotter, R., Lock, R., Enders, A., Fronzek, S., Ewert, F., 2013. Implication of crop model calibration strategies for assessing regional impacts of climate change in Europe. Agric. Forest Meteorol. 170, 32–46.
Asseng, S., Foster, I., Turner, N.C., 2011. The impact of temperature variability on wheat yields. Glob. Change Biol. 17 (2), 997–1012.
Asseng, S., Ewert, F., Rosenzweig, C., Jones, J.W., Hatfield, J.L., Ruane, A.C., Boote, K.J., Thorburn, P.J., Rotter, R.P., Cammarano, D., Brisson, N., Basso, B., Martre, P., Aggarwal, P.K., Angulo, C., Bertuzzi, P., Biernath, C., Challinor, A.J., Doltra, J., Gayler, S., Goldberg, R., Grant, R., Heng, L., Hooker, J., Hunt, L.A., Ingwersen, J., Izaurralde, R.C., Kersebaum, K.C., Mueller, C., Kumar, S.N., Nendel, C., O'Leary, G., Olesen, J.E., Osborne, T.M., Palosuo, T., Priesack, E., Ripoche, D., Semenov, M.A., Shcherbak, I., Steduto, P., Stoeckle, C., Stratonovitch, P., Streck, T., Supit, I., Tao, F., Travasso, M., Waha, K., Wallach, D., White, J.W., Williams, J.R., Wolf, J., 2013. Uncertainty in simulating wheat yields under climate change. Nat. Clim. Change 3 (9), 827–832.
Asseng, S., Ewert, F., Martre, P., Roetter, R.P., Lobell, D.B., Cammarano, D., Kimball, B.A., Ottman, M.J., Wall, G.W., White, J.W., Reynolds, M.P., Alderman, P.D., Prasad, P.V.V., Aggarwal, P.K., Anothai, J., Basso, B., Biernath, C., Challinor, A.J., De Sanctis, G., Doltra, J., Fereres, E., Garcia-Vile, M., Gayler, S., Hoogenboom, G., Hunt, L.A., Izaurralde, R.C., Jabloun, M., Jones, C.D., Kersebaum, K.C., Koehler, A.K., Mueller, C., Kumar, S.N., Nendel, C., O'Leary, G., Olesen, J.E., Palosuo, T., Priesack, E., Rezaei, E.E., Ruane, A.C., Semenov, M.A., Shcherbak, I., Stoeckle, C., Stratonovitch, P., Streck, T., Supit, I., Tao, F., Thorburn, P.J., Waha, K., Wang, E., Wallach, D., Wolf, I., Zhao, Z., Zhu, Y., 2015. Rising temperatures reduce global wheat production. Nat. Clim. Change 5 (2), 143–147.
Bassu, S., Brisson, N., Durand, J.-L., Boote, K., Lizaso, J., Jones, J.W., Rosenzweig, C., Ruane, A.C., Adam, M., Baron, C., Basso, B., Biernath, C., Boogaard, H., Conijn, S., Corbeels, M., Deryng, D., De Sanctis, G., Gayler, S., Grassini, P., Hatfield, J., Hoek, S., Izaurralde, C., Jongschaap, R., Kemanian, A.R., Kersebaum, K.C., Kim, S.-H., Kumar, N.S., Makowski, D., Mueller, C., Nendel, C., Priesack, E., Pravia, M.V., Sau, F., Shcherbak, I., Tao, F., Teixeira, E., Timlin, D., Waha, K., 2014. How do various maize crop models vary in their responses to climate change factors? Glob. Change Biol. 20 (7), 2301–2320.
Brassard, J.P., Singh, B., 2007. Effects of climate change and CO2 increase on potential agricultural production in Southern Quebec, Canada. Clim. Res. 34 (2), 105–117.
Cleland, J., 2013. World population growth; past, present and future. Environ. Resour. Econ. 55 (4), 543–554.
Daccache, A., Weatherhead, E., Stalham, M., Knox, J., 2011. Impacts of climate change on irrigated potato production in a humid climate. Agric. For. Meteorol. 151 (12), 1641–1653.
Davies, A., Jenkins, T., Pike, A., Shao, J., Carson, I., Pollock, C., Parry, M., 1997. Modelling the predicted geographic and economic response of UK cropping systems to climate change scenarios: the case of potatoes. Ann. Appl. Biol. 130 (1), 167–178.
De Temmerman, L., Hacour, A., Guns, M., 2002. Changing climate and potential impacts on potato yield and quality 'CHIP': introduction, aims and methodology. Eur. J. Agron. 17 (4), 233–242.
Devaux, A., Kromann, P., Ortiz, O., 2014. Potatoes for sustainable global food security? Potato Res. 57 (3-4), 185–199.
FAO (2016). http://faostat.fao.org/. Accessed in May 2016.
Fischer, G., van Velthuizen, H., Shah, M., Nachtergaele, F., 2002. Global Agro-ecological Assessment for Agriculture in the 21st Century: Methodology and Results 156 Ed I.-. FAO), Vienna.
Fleisher, D.H., Condori, B., Quiroz, R., Alva, A., Asseng, S., Barreda, C., Bindi, M., Boote, K.J., Ferrise, R., Franke, A.C., Govindakrishnan, P.M., Harahagazwe, D., Hoogenboom, G., Kumar, S.N., Merante, P., Nendel, C., Olesen, J.E., Parker, P.S., Raes, D., Raymundo, R., Ruane, A.C., Stockle, C., Supit, I., Vanuytrecht, E., Wolf, J., Woli, P., 2016. A potato model inter-comparison across varying climates and productivity levels, Global Change Biology. Change Biol. 3, 1258–1281.
Franke, A.C., Haverkort, A.J., Steyn, J.M., 2013. Climate change and potato production in contrasting South African agro-ecosystems 2. Assessing risks and opportunities of adaptation strategies. Potato Res. 56 (1), 51–66.
GRASS, 2012. Geographic Resources Analysis Support System (GRASS). GNU General Public Licence. http://grass.osgeo.org (Verified 04 Feb 2013).
Gbegbelegbe, S., Cammarano, D., Asseng, S., Robertson, R., Chung, U., Adam, M., Abdalla, O., Payne, T., Reynolds, M., Sonder, K., Shiferaw, B., Nelson, G., 2016. Baseline simulation for global wheat production with CIMMYT mega-environment specific cultivars. Field Crops Res. 202, 122–135.
Griffin, T.S., Bradley, S.J., Ritchie, J.T., 1993. A Simulation Model for Potato Growth and Development: SUBSTOR-potato Version 2.0. 29. Department of Aggronomy and Soil Science, College of Tropical Agriculture and Human Resources. University of Hawai, Honolulu.
Haase, N.U., Haverkort, A.J., 2006. Potato Developments in a Changing Europe. Potato Developments in a Changing Europe. 280 pp.−280 pp.
Hammes, P.S., Dejager, J.A., 1990. Net photosynthetic rate of potato at high-temperatures. Potato Res. 33 (4), 515–520.
Haris, A.A., Chhabra, V., Bhatt, B.P., Sikka, A.K., 2015. Yield and duration of potato crop in Bihar under projected climate scenarios. J. Agrometeorol. 17 (1), 67–73.
Haverkort, A., Top, J., 2011. The potato ontology: delimitation of the domain, modelling concepts, and prospects of performance. Potato Res. 54 (2), 119–136.
Haverkort, A.J., Verhagen, A., Grashoff, C., Uithol, P.W.J., 2004. POTATO-ZONING: a decision support system on expanding the potato industry through agro-ecological zoning using the LINTUL simulation approach. Decision Support Systems in Potato Production: Bringing Models to Practice. pp. 29–44.
Hijmans, R.J., Cameron, S.E., Parra, J.L., Jones, P.G., Jarvis, A., 2005. Very high resolution interpolated climate surfaces for global land areas. Int. J. Climatol. 25 (15), 1965–1978.
Hijmans, R.J., 2001. Global distribution of the potato crop. Am. J. Potato Res. 78 (6), 403–412.
Hijmans, R.J., 2003. The effect of climate change on global potato production. Am. J. Potato Res. 80 (4), 271–279.
Holden, N., Brereton, A., 2006. Adaptation of water and nitrogen management of spring barley and potato as a response to possible climate change in Ireland. Agric. Water Manage. 82 (3), 297–317.
Holden, N.M., Brereton, A.J., Fealy, R., Sweeney, J., 2003. Possible change in Irish climate and its impact on barley and potato yields? Agric. For. Meteorol. 116 (3–4), 181–196.
Hoogenboom, G., Jones, J.W., Wilkens, P.W., Porter, C.H., Boote, K.J., Hunt, L.A., Singh, U., Lizaso, J.L., White, J.W., Uryasev, O., Royce, F.S., Ogoshi, R., Gijsman, A.J., Tsuji, G.Y., Koo, J., 2015. Decision Support System for Agrotechnology Transfer (DSSAT) Version 4.6 [CD-ROM]. University of Hawaii, Honolulu, Hawaii.
IPCC, 2013. The physical science basis. In: Stocker, T.F., Qin, D., Plattner, G.-K., Tignor, M., Allen, S.K., Boschung, J., Nauels, A., Xia, Y., V, Bex, M.P.M. (Eds.), Contribution of Working Group I to the Fifth Assessment Report of the Intergovernmental Panel on Climate Change. Cambridge University Press, Cambridge, United Kingdom and New York, NY, USA, pp. 1535.
Islamov, M., 2005. Main trends in the state regulation of interactions in the seed industry sector. Mezhdunarodnyi Sel'skokhozyaistvennyi Zhurnal 5, 22–25.
Jarvis, A., Ramirez-Villegas, J., Herrera, V., Navarro-Nacines, C., 2012. Is cassava the answer to african climate change adaptation? Trop. Plant Biol. 5 (1), 9–29.
Jones, J.W., Hoogenboom, G., Porter, C.H., Boote, K.J., Batchelor, W.D., Hunt, L.A., Wilkens, P.W., Singh, U., Gijsman, A.J., Ritchie, J.T., 2003. The DSSAT cropping system model? Eur. J. Agron. 18 (3–4), 235–265.
Kalnay, E., Kanamitsu, M., Kistler, R., Collins, W., Deaven, D., Gandin, L., Iredell, M., Saha, S., White, G., Woollen, J., Zhu, Y., Chelliah, M., Ebisuzaki, W., Higgins, W., Janowiak, J., Mo, K.C., Ropelewski, C., Wang, J., Leetmaa, A., Reynolds, R., Jenne, R., Joseph, D., 1996. The NCEP/NCAR 40-year reanalysis project. Bull. Am. Meteorol. Soc. 77 (3), 437–471.
Kleinwechter, U., Gastelo, M., Ritchie, J., Nelson, G., Asseng, S., 2016. Simulating cultivar variations in potato yields for contrasting environments. Agric. Syst. 145, 51–63.
Koo, J., Dimes, J., 2015. HC27 Generic Soil Profile Database. Harvard Dataverse.
Li, T., Hasegawa, T., Yin, X., Zhu, Y., Boote, K., Adam, M., Bregaglio, S., Buis, S., Confalonieri, R., Fumoto, T., Gaydon, D., Marcaida III, M., Nakagawa, H., Oriol, P., Ruane, A.C., Ruget, F., Singh, B., Singh, U., Tang, L., Tao, F., Wilkens, P., Yoshida, H., Zhang, Z., Bouman, B., 2015. Uncertainties in predicting rice yield by current crop models under a wide range of climatic conditions. Glob. Change Biol. 21 (3), 1328–1341.
Liu, B., Asseng, S., Liu, L.L., Tang, L., Cao, W.X., Zhu, Y., 2016. Testing the responses of four wheat crop models to heat stress at anthesis and grain filling. Glob. Change Biol.

22 (5), 1890–1903.
Lutaladio, N., Castaidi, L., 2009. Potato: the hidden treasure. J. Food Compos. Anal. 22 (6).
Lutz, W., Samir, K.C., 2010. Dimensions of global population projections: what do we know about future population trends and structures? Philos. Trans. R. Soc. B-Biol. Sci. 365 (1554), 2779–2791.
Magliulo, V., Bindi, M., Rana, G., 2003. Water use of irrigated potato (*Solanum tuberosum* L.) grown under free air carbon dioxide enrichment in central ItalyWater use of irrigated potato (Solanum tuberosum L.) grown under free air carbon dioxide enrichment in central Italy. Agric. Ecosyst. Environ. 97 (1–3), 65–80.
Mahdian, M.H., Gallichand, J., 1997. Estimating potato yield with the SUBSTOR model in Quebec. Can. Agric. Eng. 39 (3), 157–164.
Mendoza, H.A., Haynes, F.L., 1976. Variability for photoperiodic reaction among diploid and tetraploid potato clones from three taxonomic groups. Am. Potato J. 53 (9), 319–332.
Monfreda, C., Ramankutty, N., Foley, J.A., 2008. Farming the planet: 2. Geographic distribution of crop areas, yields, physiological types, and net primary production in the year 2000. Glob. Biogeochem. Cycles 22 (1), 19.
Mueller, C., Robertson, R.D., 2014. Projecting future crop productivity for global economic modeling. Agric. Econ. 45 (1), 37–50.
Mueller, N., Gerber, J., Johnston, M., Ray, D., Ramankutty, N., Foley, J., 2012. Closing yield gaps through nutrient and water management. Nature 490 (7419), 254–257.
Raymundo, R., Asseng, S., Cammarano, D., Quiroz, R., 2014. Potato sweet potato, and yam models for climate change: a review. Field Crops Res. 166, 173–185.
Raymundo, R., Asseng, A., Prasad, R., Kleinwechter, U., Concha, J., Condori, B., Bowen, W., Wolf, J., Olesen, J.E., Dong, Q., Zotarelli, L., Gastelo, M., Alva, A., Travasso, M., Quiroz, R., Arora, V., Graham, W., Porter, C., 2016. Performance of the SUBSTOR-potato model across contrasting growing conditions. Field Crops Res. 202, 57–76.
Ritchie, J.T., Griffin, T.S., Johnson, B.S., 1995. SUBSTOR: Functional model of potato growth, development and yield. Modelling and Parameterization of the Soil-Plant-Atmosphere System: A Comparison of Potato Growth Models. pp. 401–435.
Sanabria, J., Lhomme, J., 2013. Climate change and potato cropping in the Peruvian Altiplano? Theor. Appl. Climatol. 112 (3–4), 683–695.
Shae, J.B., Steele, D.D., Gregor, B.L., 1999. Irrigation scheduling methods for potatoes in the northern great plains. Trans. ASAE 42 (2), 351–360.
Siebert, S., Kummu, M., Porkka, M., Doll, P., Ramankutty, N., Scanlon, B.R., 2015. A global data set of the extent of irrigated land from 1900 to 2005. Hydrol. Earth Syst. Sci. 19 (3), 1521–1545.
Singh, J.P., Govindakrishnan, P.M., Lal, S.S., Aggarwal, P.K., 2005. Increasing the efficiency of agronomy experiments in potato using INFOCROP-POTATO model. Potato Res. 48, 131–152.
Snapp, S.S., Fortuna, A.M., 2003. Predicting nitrogen availability in irrigated potato systems. Horttechnology 13 (4), 598–604.
St'astna, M., Toman, F., Dufkova, J., 2010. Usage of SUBSTOR model in potato yield prediction. Agric. Water Manage. 97 (2), 286–290.
Stockle, C.O., Donatelli, M., Nelson, R., 2003. CropSyst: a cropping systems simulation model. Eur. J. Agron. 18 (3–4), 289–307.
Stockle, C.O., Nelson, R.L., Higgins, S., Brunner, J., Grove, G., Boydston, R., Whiting, M., Kruger, C., 2010. Assessment of climate change impact on eastern Washington agriculture? Clim. Change 102 (1–2), 77–102.
Stoorvogel, J., Antle, J., Crissman, C., Bowen, W., 2004. The Tradeoff analysis model: integrated bio-physical and economic modeling of agricultural production systems. Agric. Syst. 80 (1), 43–66.
Streck, N.A., de Paula, F.L.M., Bisognin, D.A., Heldwein, A.B., Dellai, J., 2007. Simulating the development of field grown potato (*Solanum tuberosum* L.). Agric. Forest Meteorol. 142 (1), 1–11.
Supit, I., van Diepen, C., de Wit, A., Wolf, J., Kabat, P., Baruth, B., Ludwig, F., 2012. Assessing climate change effects on European crop yields using the Crop Growth Monitoring System and a weather generator. Agric. For. Meteorol. 164, 96–111.
Theisen, K., Thiele, G., 2008. Implementing CIP's vision: impact targeting. In: Social Sciences Working Paper. 46 Lima – Peru: International Potato Center.
Travasso, M.I., Caldiz, D.O., Saluzzo, J.A., 1996. Yield prediction using the SUBSTOR-potato model under Argentinian conditions. Potato Res. 39 (3), 305–312.
Tubiello, F.N., Rosenzweig, C., Goldberg, R.A., Jagtap, S., Jones, J.W., 2002. Effects of climate change on US crop production: simulation results using two different GCM scenarios. Part I: wheat, potato, maize, and citrus. Clim. Res. 20 (3), 259–270.
Webber, H., Zhao, G., Wolf, J., Britz, W., de Vries, W., Gaiser, T., Hoffmann, H., Ewert, F., 2015. Climate change impacts on European crop yields: do we need to consider nitrogen limitation? Eur. J. Agron. 71, 123–134.
White, J.W., Hoogenboom, G., Kimball, B.A., Wall, G.W., 2011. Methodologies for simulating impacts of climate change on crop production. Field Crops Res. 124 (3), 357–368.
You, L.Z., Wood, S., Wood-Sichra, U., Wu, W.B., 2014. Generating global crop distribution maps: from census to grid. Agric. Syst. 127, 53–60.
Zhao, G., Hoffmann, H., Yeluripati, J., Xenia, S., Nendel, C., Coucheney, E., Kuhnert, M., Tao, F.L., Constantin, J., Raynal, H., Teixeira, E., Grosz, B., Doro, L., Kiese, R., Eckersten, H., Haas, E., Cammarano, D., Kassie, B., Moriondo, M., Trombi, G., Bindi, M., Biernath, C., Heinlein, F., Klein, C., Priesack, E., Lewan, E., Kersebaum, K.C., Rotter, R., Roggero, P.P., Wallach, D., Asseng, S., Siebert, S., Gaiser, T., Ewert, F., 2016. Evaluating the precision of eight spatial sampling schemes in estimating regional means of simulated yield for two crops. Environ. Modell. Softw. 80, 100–112.